Virology 381 (2008) 268–276

Contents lists available at ScienceDirect

Virology

journal homepage: www.elsevier.com/locate/yviro

Identification of genetic determinants of a tick-borne flavivirus associated with host-specific adaptation and pathogenicity

Dana N. Mitzel [a], Sonja M. Best [a], Max F. Masnick [a], Stephen F. Porcella [b], James B. Wolfinbarger [a], Marshall E. Bloom [a,*]

[a] Laboratory of Virology, Rocky Mountain Laboratories, National Institute of Allergy and Infectious Diseases, National Institutes of Health, 903 South Fourth Street, Hamilton, MT 59840, USA
[b] Genomics Unit Research Technologies Section, Rocky Mountain Laboratories, National Institute of Allergy and Infectious Diseases, National Institutes of Health, 903 South Fourth Street, Hamilton, MT 59840, USA

ARTICLE INFO

Article history:
Received 11 July 2008
Returned to author for revision
5 August 2008
Accepted 19 August 2008
Available online 26 September 2008

Keywords:
Tick-borne flavivirus
Langat virus
Genetic correlates
Replication
Neuroinvasiveness
Attenuation

ABSTRACT

Tick-borne flaviviruses are maintained in nature in an enzootic cycle involving a tick vector and a vertebrate host. Thus, the virus replicates in two disparate hosts, each providing selective pressures that can influence virus replication and pathogenicity. To identify viral determinants associated with replication in the individual hosts, plaque purified Langat virus (TP21pp) was adapted to growth in mouse or tick cell lines to generate two virus variants, MNBp20 and ISEp20, respectively. Virus adaptation to mouse cells resulted in four amino acid changes in MNBp20 relative to TP21pp, occurring in E, NS4A and NS4B. A comparison between TP21pp and ISEp20 revealed three amino acid modifications in M, NS3 and NS4A of ISEp20. ISEp20, but not MNBp20, was attenuated following intraperitoneal inoculation of mice. Following isolation from mice brains, additional mutations reproducibly emerged in E and NS3 of ISEp20 that were possibly compensatory for the initial adaptation to tick cells. Thus, our data implicate a role for E, M, NS3, NS4A and NS4B in host adaptation and pathogenicity of tick-borne flaviviruses.

Published by Elsevier Inc.

Introduction

Flaviviruses cause globally significant emerging diseases and include tick-borne encephalitis virus (TBEV), Japanese encephalitis virus, West Nile virus (WNV), dengue virus and yellow fever virus (YFV). The 11 kb single-stranded RNA genome of flaviviruses encodes a single large polyprotein flanked by 5′ and 3′ untranslated regions (UTR) of variable sizes. Following translation, the viral polyprotein is cleaved by host and viral proteases into ten proteins: three structural proteins [capsid (C), membrane (M; derived from its precursor, prM) and envelope (E)] and seven nonstructural proteins (NS1, NS2A, NS2B, NS3, NS4A, NS4B and NS5) (Lindenbach and Rice, 2001). Several viruses belong to the TBEV serogroup, including Omsk hemorrhagic fever virus, Kyasanur Forest disease virus, Powassan virus and Langat virus (LGTV). The tick-borne flaviviruses cause a range of clinical findings following infection of humans, from mild febrile forms to severe, sometimes fatal, meningoencephalitis and hemorrhagic fever (Gritsun et al., 2003). In spite of the distinct clinical syndromes, the genetic basis for differences in pathogenicity of these closely related viruses is poorly understood.

In nature, tick-borne flaviviruses are maintained through a transmission cycle involving an ixodid tick vector and a vertebrate host. Once infected, virus can persist in ticks for the remainder of the tick's life span, enabling virus transmission for years after the initial infection (Chernesky and McLean, 1969; Costero and Grayson, 1996; Nuttall and Labuda, 2003). For this reason, ticks not only make efficient virus reservoirs, but also exert long-term selective pressures that may influence virus genotype and phenotype (Dzhivanian et al., 1988; Labuda et al., 1994; Nuttall et al., 1991). In support of this theory, a correlation between virus pathogenicity and the distribution of specific tick species has been identified (Leonova, 1997). Hence, persistence in ticks may select virus populations and thus influence virus virulence in the accidental human host.

The primary vertebrate hosts for the medically important tick-borne flaviviruses are small rodents (Nuttall and Labuda, 1994). In contrast to ticks, mammalian hosts function as short-lived reservoirs and infections are generally of limited duration. Although the majority of the virus's evolutionary lifespan is spent in the tick vector, transmission to a vertebrate host is required to ensure survival in nature (Gritsun et al., 2003; Nuttall and Labuda, 2003). Consequently, the requirement for sufficient virus replication in the mammalian

* Corresponding author. Laboratory of Virology, Rocky Mountain Laboratories, NIAID, NIH Hamilton, MT 59840, USA. Fax: +1 406 375 9620.
E-mail addresses: dmitzel@niaid.nih.gov (D.N. Mitzel), mbloom@niaid.nih.gov (M.E. Bloom).

0042-6822/$ – see front matter. Published by Elsevier Inc.
doi:10.1016/j.virol.2008.08.030

host to ensure transmission must also exert selective pressure on the virus population (Gritsun et al., 2003; Kaluzova et al., 1994).

The viral determinants specifically required for replication in a tick or vertebrate host are not well defined. Due to roles in receptor binding and membrane fusion, the E protein is an important viral determinant of cell tropism (Kaluzova et al., 1994; Labuda et al., 1994; Romanova et al., 2007). In addition, the 3′ UTR is a host-specific determinant of replication and may influence vector specificity and virulence (Alvarez et al., 2005; Bryant et al., 2005; Gritsun and Gould, 2006; Yu and Markoff, 2005; Zeng et al., 1998). However, it is unknown if additional areas of the genome are important for host adaptation. Furthermore, how selection for these determinants in one host influences replication and pathogenesis in the alternative host in the transmission cycle is not well understood.

The aim of this study was to identify genetic determinants within the tick-borne flavivirus genome important for replication in either the tick or the mammalian host. Plaque purified LGTV was serially passed in two distinct cell lines, mouse neuroblastoma cells (MNB-509) or tick *Ixodes scapularis* embryonic cells (ISE6), to obtain two virus variants. Various properties of the variants including viral RNA replication, neurovirulence and neuroinvasiveness were examined. Genetic mutations associated with changes in these properties were identified by sequencing the viral genome. Genetic substitutions in two distinct regions of the genome were found to be correlated with adaptation to growth in mammalian or tick hosts. The first region was the structural proteins (M and E) and the second distinct area encompassed NS3, NS4A and NS4B. Hence, this study implicated a role for both the nonstructural proteins and the structural proteins in host adaptation of tick-borne flaviviruses.

Results

Adaptation of Langat virus following serial passage in mammalian and tick cells

We sought to identify areas of the genome important for virus replication within mammalian or tick hosts. Two viral variants (MNBp20 and ISEp20) were created by 20 serial passages of plaque purified LGTV (TP21pp) in either MNB or ISE6 cells, respectively. When titered in Vero cells, a phenotypic change was observed for MNBp20 (Fig. 1). This variant demonstrated a significantly smaller ($p<0.05$) focus size compared to the focus diameter of TP21pp. In contrast, the focus size of ISEp20 did not differ from TP21pp on Vero cells. Thus, this phenotypic change observed for MNBp20 suggested that serial passage of TP21pp in MNB cells resulted in restricted virus spread in Vero cells.

To determine if virus adaptation to individual cell lines had occurred during serial passage, the kinetics of RNA replication for TP21pp, MNBp20 or ISEp20 were examined in MNB or ISE6 cells by real-time PCR. Quantification of the fold difference in RNA was determined by normalizing viral RNA to an endogenous control at each time point and using the data at 0 h post infection (hpi) as the reference point. Efficiency of RNA replication for TP21pp and ISEp20 was similar in MNB cells (Fig. 2A). By 72 hpi, the levels of RNA for both ISEp20 and TP21pp increased approximately 0.6 logs above the 0 hpi time point. In contrast, MNBp20 replicated to higher levels than TP21pp throughout the time course (Fig. 2A). Greater RNA replication efficiency of MNBp20 could be detected as early as 12 hpi and by 72 hpi the amount of MNBp20 RNA increased approximately 3.5 logs compared to 0 hpi. These results suggested that serial passage of TP21pp in MNB cells led to emergence of a virus variant (MNBp20) with enhanced RNA replication in this cell line.

Following infection of ISE6 cells, ISEp20 RNA replication was more efficient than that of MNBp20 or TP21pp (Fig. 2B). A difference in the level of RNA replication was identified by 24 hpi, at which time a 1.8 log increase was observed in ISEp20 RNA compared to the 0.8 log increase in TP21pp RNA. By 72 hpi, the level of ISEp20 RNA was approximately 4 logs greater than the input RNA at 0 hpi. In comparison, TP21pp and MNBp20 exhibited a 2.8 and a 1.5 log increase over input RNA, respectively. These results suggested that virus passaged in tick cells led to a specific adaption of ISEp20 replication in ISE6 cells. In addition, adaptation to MNB cells resulted in impaired RNA replication of MNBp20 in ISE6 cells relative to TP21pp. Taken together, these data established that the virus passaged in mouse or tick cells adapted to growth in the specific cell lines.

Altered neuroinvasiveness of ISEp20 in C57Bl/6 mice

To determine if adaptation to the individual cell types resulted in altered virus virulence, cell-derived variants were inoculated into three week old C57Bl/6 mice. The pathogenicity of tick-borne flaviviruses involves two distinct parameters, neurovirulence and neuroinvasiveness. Neurovirulence was examined by intracranial (IC) inoculation and neuroinvasiveness was assessed by intraperitoneal (IP) inoculation. Following IC inoculation, the median survival time and the survival rate were similar among mice inoculated with TP21pp, MNBp20, and ISEp20, with no significant difference identified among the survival curves (Fig. 3A). These data

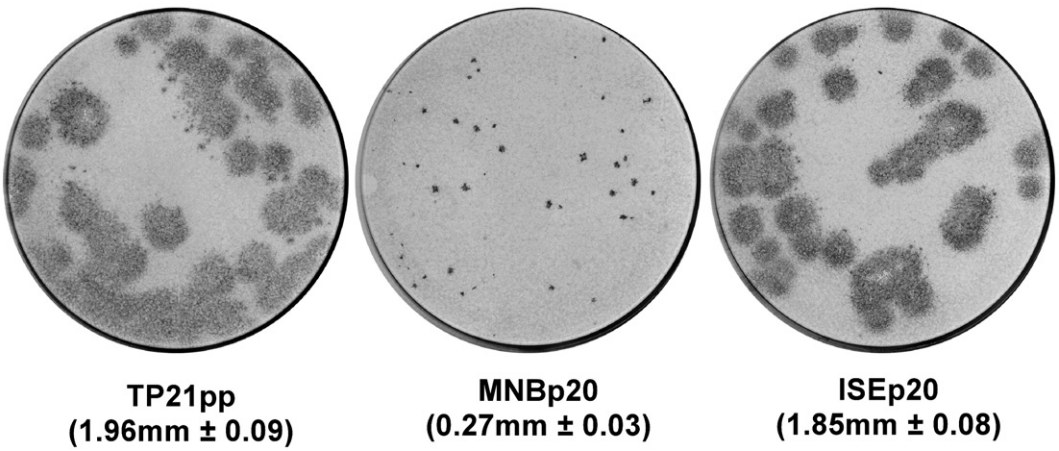

Fig. 1. Focus morphology of cell-derived variants and TP21pp. Vero cells were infected with plaque purified virus (TP21pp), MNB cell-derived variant (MNBp20), and tick cell-derived variant (ISEp20) and overlaid with 0.8% methylcellulose. At 4 dpi, cells were fixed with 100% methanol and the foci were visualized using immunoperoxidase staining. The mean foci diameter (±standard error of the mean or SEM) for each virus is indicated.

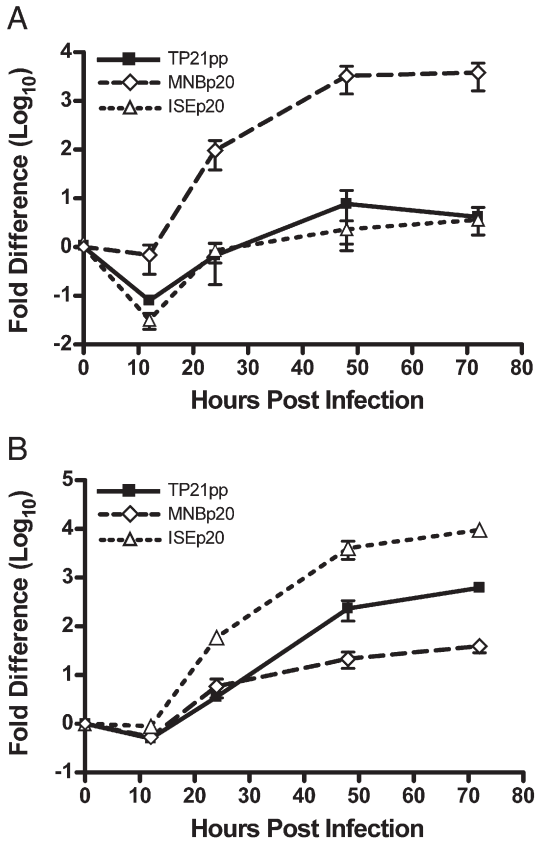

Fig. 2. RNA replication kinetics of TP21pp, MNBp20, and ISEp20 in MNB and ISE6 cells. Total RNA was isolated from (A) MNB cells or (B) ISE6 cells infected with parental virus (TP21pp) or its two variants, MNBp20 or ISEp20 at 0, 12, 24, 48, and 72 hpi. Real-time PCR was used to quantitate the changes in the positive sense strands of viral RNA. Data at each timepoint were normalized to the endogenous controls: eukaryotic 18s rRNA for MNB cell infection or *I. scapularis* 16s rRNA for ISE6 cell infection. The data obtained at 0 hpi were used as the reference point for determining the fold difference. The mean ± SEM was obtained from three independent experiments.

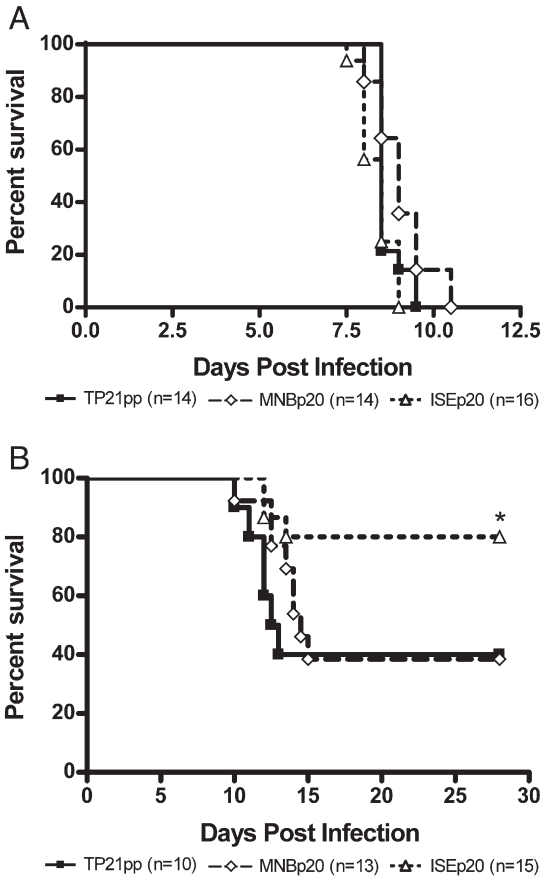

Fig. 3. Effects of cell adaptation on virulence in 3 week old C57Bl/6 mice. Mice were inoculated (A) intracranially with 100 ffu or (B) intraperitoneally with 1000 ffu of TP21pp, MNBp20, or ISEp20. Mice were observed daily for neurological signs and animals demonstrating hind-limb paralysis were considered terminal. Percent survival is plotted as a function of time in days post infection (dpi). The number of mice in each group is indicated (*n*). Asterisk (*) indicates a significant difference (*p* value = 0.0274) from TP21pp.

suggest that adaptation to mouse or tick cells did not alter the neurovirulence of the virus variants.

In contrast to the results following IC inoculation, a difference in neuroinvasiveness was observed following IP inoculation. Mice inoculated IP with TP21pp had a survival rate of 40%, with a median survival time of 12.75 days. No statistical significance was demonstrated between the survival curves for MNBp20 and TP21pp (*p* value = .6045). In contrast, a significantly higher (*p* = 0.0274) survival rate of 80% was observed in mice inoculated IP with ISEp20 when compared to TP21pp (Fig. 2B). Since several mice survived to 28 dpi, we sought evidence of subclinical infection by examining the sera of these mice for the presence of LGTV-specific antibody. All surviving mice, regardless of viral inoculum, seroconverted (data not shown) demonstrating that the decrease in neuroinvasivesness of ISEp20 was not a reflection of decreased infectivity following IP inoculation. These data suggested that adaptation of TP21pp to tick cells was associated with reduced neuroinvasiveness in mice following IP inoculation.

Flavivirus attenuation is often associated with a small plaque phenotype on various mammalian cells, including Vero cells (Blaney et al., 2002; Butrapet et al., 2000; Lee et al., 2004; Pletnev, 2001; Pletnev and Men, 1998). Since attenuation of MNBp20 was not observed following inoculation of mice, we were concerned that reversion of MNBp20 to a large focus phenotype may have occurred as observed in previous studies (Puig-Basagoiti et al., 2007). However, virus isolated from the brains of the moribund mice inoculated with MNBp20 maintained the small focus phenotype when titered on Vero cells (data not shown), suggesting that reversion had not occurred. Thus, although adaptation to replication in MNB cells resulted in restricted replication in both Vero and ISE6 cells, it was not associated with altered pathogenicity in mice.

Sequence changes associated with adaptation to mouse or tick cell lines

The results described above demonstrated that passage of virus in either tick or mammalian cell lines resulted in virus adaptation to replication within those cells. However, only adaptation to growth in tick cells resulted in altered neuroinvasiveness in mice, suggesting that different mutations may have arisen in the two virus variants. To identify genetic changes associated with adaptation, the entire viral genome of approximately 11 kb, except for the last 20 nucleotides at the 3′ terminus, was sequenced for the two virus variants and TP21pp.

Few alterations were identified in the consensus sequence of the variants following 20 serial passages in either cell line when compared to TP21pp (Table 1). Analysis of the MNBp20 sequence demonstrated 4 nucleotide modifications, representing 4 non-synonymous changes.

Table 1
Changes in nucleotides and amino acids of MNBp20 and ISEp20 following adaptation to cell culture

	MNBp20				ISEp20		
Protein	E	E	NS4A	NS4B	M	NS3	NS4[a]
Nucleotide	g1799a	t2282y	a6558g	a7398r	a821g	t6407y	c6702y
Amino acid	E277K	Y438Y/H[a]	E33G	K164K/R[a]	K115E	F604F/L[a]	A81A/V[a]

[a] The presence of multiple nucleotides at a single loci resulted in quasispecies containing two amino acids.

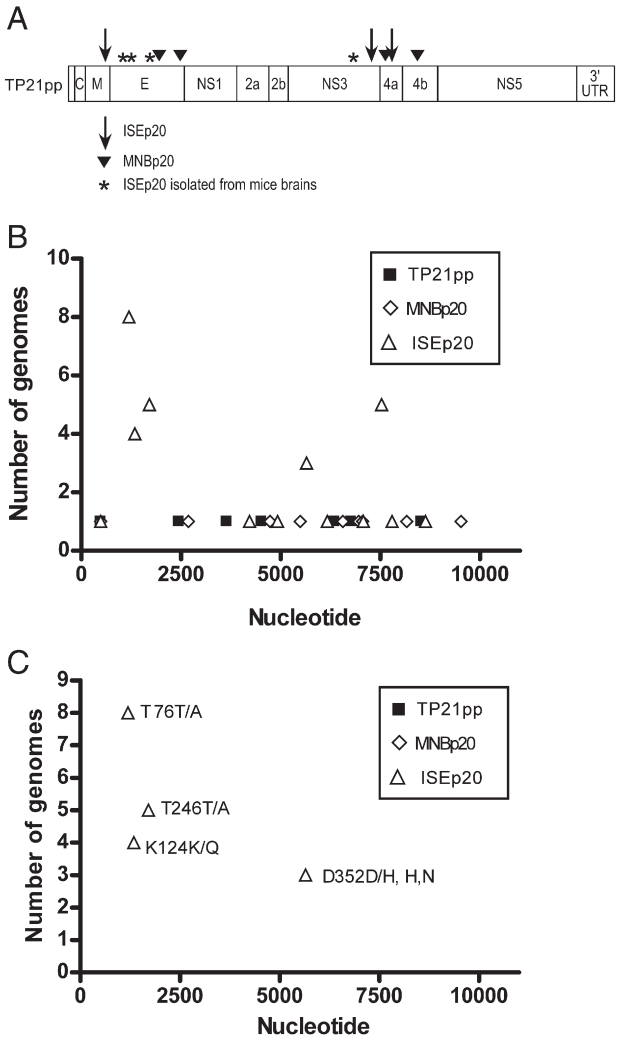

Fig. 4. Genotypic changes of TP21pp, MNBp20, and ISEp20 following a single passage in mice. Two and three week old C57Bl/6 mice were inoculated intracranially and intraperitoneally with TP21pp, MNBp20, or ISEp20. Total RNA was isolated from brains of moribund mice and the viral genome was sequenced. (A) The schematic represents the sequence obtained for TP21pp. Amino acid changes following cell culture adaptation are depicted by an arrowhead for MNBp20 or an arrow for ISEp20. The reproducible amino acid variations that occurred in ISEp20 following passage in mice are denoted by asterisks (*). (B) Total nucleotide changes identified in virus variants and TP21pp. (C) Amino acid changes identified in TP21pp, MNBp20, and ISEp20 that occurred in multiple mice. The amino acid substitution is labelled. The *x*-axis in B and C represents nucleotide location in the virus genome (10943 total nucleotides). The *y*-axis denotes the number of mice in which the mutation was identified.

Two amino acid variations (E277K and Y438Y/H) were identified in the E protein and two changes were identified in the nonstructural proteins NS4A (E33G) and NS4B (K164K/R). Numbering for the amino acid variations is in relation to the individual proteins. Multiple peaks were identified in sequencing results at nucleotides t2282y and a7398r suggesting the presence of a quasispecies at amino acids Y438Y/H and K164K/R, respectively. In addition, the modifications occurring at amino acids E277K, Y438Y/H, and E33G altered the charge at these residues.

Following 20 passages in ISE6 cells, three nucleotide changes resulting in non-synonymous amino acid alterations were identified in ISEp20 relative to TP21pp. These variations were identified in the structural protein, M (K115E), and in the nonstructural proteins NS3 (F604F/L) and NS4A (A81A/V). Quasispecies were identified at amino acids F604F/L and A81A/V. Only the genetic change occurring at amino acid K115E demonstrated a non-conserved modification resulting in a charge difference.

To determine if the mutations identified in MNBp20 and ISEp20 arose early or late in the passage history, the viral genomes of intermediate passages (passage 6 and 12) were sequenced (data not shown). This revealed that the K115E (M protein) mutation in ISEp20 occurred between passage 7 and 12 and the substitution, E227K, in the E protein of MNBp20 arose within the first 6 passages. All other mutations identified for the two variants surfaced following the twelfth passage of TP21pp in the respective cell lines.

Interestingly, the variations found in MNBp20 and ISEp20 were identified in the same two areas of the genome (Fig. 4A). The first region was located in the structural proteins, M and E, and the second area encompassed the nonstructural proteins, NS3, NS4A and NS4B. Thus, in addition to the known role of E in cell tropism, these data suggested a possible involvement of the nonstructural proteins in host adaptation.

Sequence changes following passage in mice

The results described in the previous section demonstrated that adaptation of TP21pp to tick cells, but not to MNB cells, resulted in altered neuroinvasiveness in mice. However, as shown in Fig. 1, the emergence of MNBp20 was associated with a small focus phenotype that was maintained through one passage in mice with no measurable difference in virus virulence. This unexpected result prompted us to determine if additional genetic changes occurred during replication in mice. Viral RNA was isolated from the brains of 28 moribund mice infected with TP21pp, MNBp20 or ISEp20. The RNA was amplified and sequenced as described above and the sequences were compared with the input virus.

Following passage in mice, a total of 47 nucleotide changes were identified in TP21pp and the cell adapted variants (Fig. 4B). Most of these changes occurred only once and were spread across the genome regardless of the virus inoculum, suggesting that these substitutions may represent random changes. To identify genomic changes that could represent positive selection, we focused on specific amino acid substitutions that reproducibly occurred in multiple mice (Fig. 4C and Table 2). When we applied this constraint, we found no reproducible genetic modifications in the sequence of either MNBp20 or TP21pp. In addition, the original mutations contained within MNBp20 were maintained through a single passage in mice. Thus, these data implied that the residue changes identified following passage in MNB cells were stable.

In contrast, reproducible amino acid modifications were detected in the genome of virus isolated from mice inoculated with ISEp20. In total, viral RNA was isolated and sequenced from 11 mice. Three out of the four identified changes (T76T/A, K124K/Q, T246T/A) were situated in the E protein. The two most frequent coding changes were located at amino acid 76 (8/11 mice) and 246 (5/11 mice). The fourth amino acid substitution was located in NS3 (D352D/H,H,N) and occurred in 3 of 11 mice. Although the sequence at residue 352 was different in all three mice, the modifications identified all resulted in an amino acid charge difference.

Table 2
Recurring genomic changes identified in ISEp20 following a single passage in mice

Protein	Nucleotide	Amino acid
E[a]	a1196g	T76A
	a1196r	T76T/A[b]
E	a1340m	K124K/Q[b]
E	a1706r	T246T/A[b]
NS3[a]	g5651s	D352D/H[b]
	g5651c	D352H
	g5651a	D352N

[a] The variations noted at a single residue are due to differences in the sequence of the viral genomes isolated from individual mice.
[b] The presence of multiple nucleotides at a single loci resulted in quasispecies containing two amino acids.

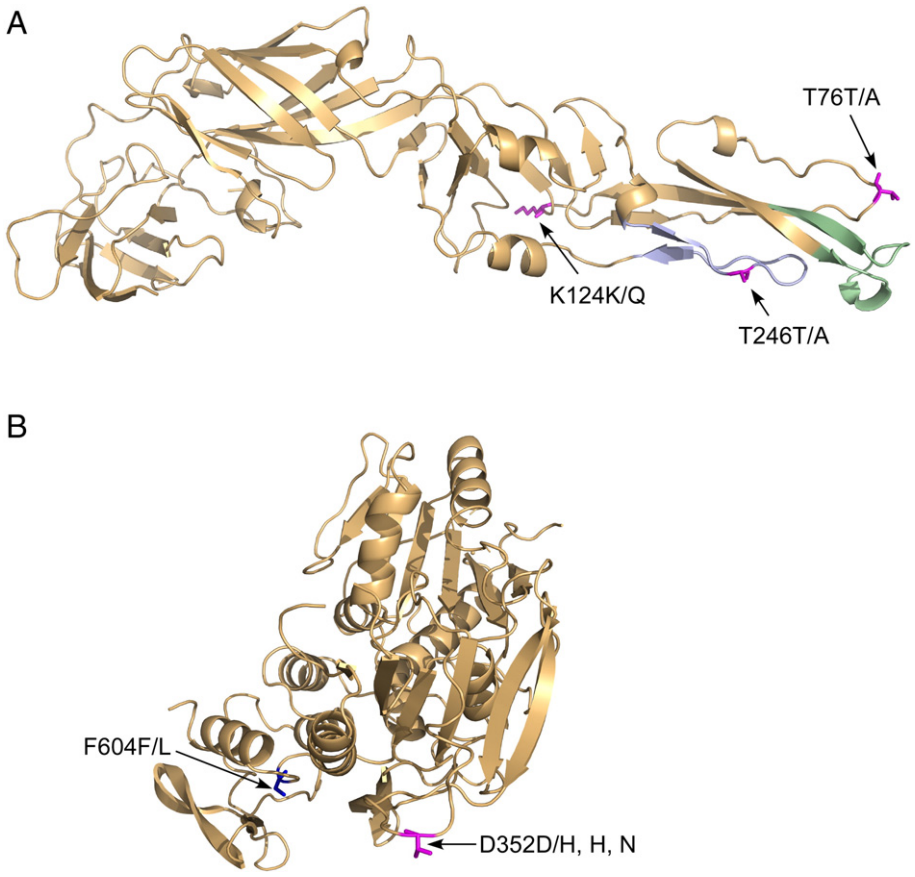

Fig. 5. Modelling of amino acid substitutions within ISEp20 on the three-dimensional structures of E and NS3. (A) Amino acid substitutions in the E protein of ISEp20 following passage in mice (pink) were aligned and modelled on E from TBEV. The fusion peptide (light green) and the ij loop (light blue) are indicated. (B) Amino acid changes identified in ISEp20 NS3 following tick cell adaptation (blue) or passage in mice (pink) were mapped to homologous sequences on the structure of the YFV NS3 helicase domain. The numbering and residue substitutions are labeled on each structure.

It is noteworthy that the mutations arising in both the E and NS3 proteins of ISEp20 isolated from mice were proximal in the linear sequence to the original mutations identified following adaptation to replication in tick cells (Fig. 4A). To further understand the relationship between these residues, we modeled them on the three-dimensional crystal structures of TBEV E and YFV NS3 (Rey et al., 1995; Wu et al., 2005). The two mutations occurring most frequently in E, T76T/A and T246T/A, were positioned proximal to the fusion peptide (Fig. 5A). T246T/A lies within the ij loop of E (Rey et al., 1995; Yamashita et al., 2008). This loop is suggested to interact with the N-terminus of M that may include the original mutation in ISEp20 at K115E. This possibility is explored further in the discussion. The mutations in NS3, F604F/L (in ISEp20) and D352D/H,H,N (in ISEp20 following one passage in mice) are both located in the putative RNA binding cleft of the flavivirus helicase (Wu et al., 2005; Yamashita et al., 2008) (Fig. 5B). Given that mutations were not observed in MNBp20 isolated from mice, these data suggest that changes in ISEp20 were not a consequence of tissue culture adaptation in general, but were more likely compensatory for the initial adaptation to the tick cell line. These data further implicate the nonstructural proteins as well as the structural proteins as important viral determinants for host adaptation and neuroinvasion of the virus.

Discussion

Persistence of tick-borne flaviviruses in nature requires these viruses to replicate in two distinct hosts (arthropod and vertebrate). Selection of viruses during replication in specific tick species may influence pathogenesis following infection of humans (Leonova, 1997). One strategy to understand how the host influences virus replication and pathogenesis is to identify viral determinants that confer a replication advantage in a host-specific manner and then examine how these determinants influence pathogenesis. To identify potential viral determinants important for replication in tick and mammalian hosts, we serially passed plaque purified LGTV (TP21pp) in either tick ISE6 or mouse MNB cells. The resulting virus variants, ISEp20 and MNBp20, were specifically adapted to replication in their respective cell type (Fig. 2) suggesting that genetic changes occurring in these viruses may represent host-specific determinants of replication. Specifically, amino acid changes were identified in the nonstructural proteins, NS3, NS4A and NS4B, in addition to the structural proteins, M and E. Hence, these proteins may have host-specific roles in replication of tick-borne flaviviruses and thus may be important for host adaptation.

Virus adapted to tick cells (ISEp20) had reduced neuroinvasiveness following IP inoculation of mice which was associated with three amino acid modifications (one each in M, NS3 and NS4A) (Fig. 4A and Table 1). Following isolation from the brains of mice, the genome of ISEp20 contained a number of additional mutations that reproducibly emerged in E and NS3 (Fig. 4 and Table 2). Strikingly, these mutations were in areas of the genome proximal to the mutations originally identified following cell adaptation (Figs. 4A and 5). Together with the observation that ISEp20 was the only virus variant with reproducibly occurring mutations in mice, this finding suggests that the mutations arising in mice were likely compensatory for the initial adaptation to tick cell culture. This interpretation is supported by multiple existing studies. The K115E (of prM, or the 26th amino acid of M) mutation lies adjacent to a region of M that modulates E protein function during

early steps of infection such as membrane fusion (Maier et al., 2007). Additional structural studies of the M and E proteins suggest that the first approximately 20 residues of the M protein interact with the ij loop in domain II (dimerization and fusion domain) of E (Zhang et al., 2003). The two most frequent mutations arising after mouse passage (at amino acids 76 and 246) were located near the fusion peptide with T246T/A substitution occurring in the ij loop. Furthermore, K124K/Q lies in a region important for determining the pH at which acid-induced conformation changes needed for membrane fusion occur. Taken together, these studies suggest that K115E of ISEp20 M may modulate membrane fusion in a host-specific manner and that the mutations in domain II of E were selected following passage in mice to compensate for the original K115E mutation. It is possible that a similar host-specific selection and subsequent compensation has influenced ISEp20 NS3, since both mutations in NS3, F604F/L (in ISEp20) and D352D/H,H,N (in ISEp20 following passage in mice), are located in the putative RNA binding cleft of the helicase domain (Wu et al., 2005; Yamashita et al., 2008).

The adaptation of ISEp20 to more efficient RNA replication in tick cells did not result in impaired RNA replication in the mammalian cell line. However, ISEp20 was clearly attenuated in mice following IP inoculation. Thus, the mutations identified in ISEp20 were not determinants of replication in mouse cells but were determinants of neuroinvasion in the mouse. This suggested that viral determinants of replication and neuroinvasiveness can be separated from each other. This is a significant observation because most amino acid mutations in flaviviruses that affect pathogenesis are associated with reduced replication in tissue culture (Chiou and Chen, 2001; Rossi et al., 2007; Rumyantsev et al., 2006b; Wicker et al., 2006) thus providing an explanation for virus attenuation. Limited quantities of virus stocks precluded us from completing additional experiments to clearly define the pathogenesis of our virus variants in mice. However, we can now use reverse genetics to thoroughly test the hypothesis that the individual mutations in M, NS3 and NS4A arising in ISEp20 are tick-specific determinants of replication as well as determinants of pathogenesis.

Following adaptation to MNB cells, MNBp20 demonstrated a small focus phenotype when titered in Vero cells relative to the parental plaque purified virus, TP21pp. (Fig. 1) Genetic correlates for this phenotypic change were identified in E, NS4A and NS4B (Table 1). Viruses with a small plaque phenotype are usually sought after for vaccine candidates since this phenotype is often associated with attenuation in animals (Blaney, et al., 2002; Butrapet et al., 2000; Lee et al., 2004; Pletnev, 2001; Rumyantsev et al., 2006b). However, despite its restricted growth in Vero cells, MNBp20 demonstrated similar neurovirulence and neuroinvasiveness to TP21pp in mice. In addition, mutations in MNBp20 were also associated with an increase in RNA replication efficiency in MNB cells (Fig. 2A). A correlation between reduction of virus replication in neural cells and virus attenuation *in vivo* has been described for flaviviruses (Chiou and Chen, 2001; Rumyantsev et al., 2006a; Rumyantsev et al., 2006b). However, the converse did not occur; the increase in MNBp20 replication in MNB cells was not a predictor for a more neurovirulent virus *in vivo*. Thus, we can not rule out the possibility that despite the similar neurovirulence, differences in virus replication among the virus variants *in vivo* could occur.

Relatively few changes were identified following adaptation of TP21pp to either MNB or ISE6 cells. The complete sequence was obtained for all but the last 20 nucleotides at the 3′ terminus. Thus, the possibility that mutations might have occurred in this area and that these substitutions could have an affect on host adaptation, virus replication and neuroinvasiveness can not be entirely dismissed. However, we believe that E, prM, NS3, NS4A and NS4B proteins are important to host adaptation because amino acid substitutions in the areas described here for LGTV have been obtained for other tick-borne and mosquito-borne flaviviruses. Romanova et al. identified genetic differences in prM, E, NS2A and NS4A when comparing a tick-borne flavivirus derived following passage in ticks or in mice brains (Romanova et al., 2007). The differences occurred at remarkably similar positions to those arising in our viruses. In particular, a tick-adapted virus clone derived in pig embryo kidney (PEK) cells contained a mutation at E residue K124 which was at the same position as K124K/Q in ISEp20 isolated from mice brains. Furthermore, an amino acid substitution in E associated with a small plaque phenotype was identified 12 residues from Y438Y/H found in MNBp20, and two mutations were observed in NS4A that flank E33G in MNBp20 by approximately 10 amino acids on either side. In addition to the mutations identified in tick-borne viruses, amino acid substitutions in E, prM, NS4A and NS4B were obtained following passage of WNV and Saint Louis encephalitis virus (SLEV) in mosquito cells (Ciota et al., 2007a). Hence, these studies suggest that alterations in E, prM, NS4A and NS4B are more generally reproducible and that these proteins may be determinants involved in host-specific replication of flaviviruses.

Ciota et al. implicated an amino acid change in NS4A as having a major role in the increased replication fitness of both WNV and SLEV variants in mosquito cells (Ciota et al., 2007a). Despite these findings, introduction of this NS4A mutation into a WNV molecular clone had negligible affects on virus replication in cell culture (Ciota et al., 2007b). Thus, the cell-specific replicative advantage of cell-culture adapted virus variants observed by these investigators is not likely to result solely from consensus changes in amino acid sequences. Minority populations and perhaps synonymous alterations in the RNA sequence affecting secondary structure may be important in the adaptive genotype and phenotype of the passaged population. In support of this hypothesis, long-term transmission of a defective dengue virus genome in humans occurred most likely through trans-complementation with functional viruses (Aaskov et al., 2006). Furthermore, studies of polio virus determined a requirement for quasispecies generation and their cooperative interactions in virus pathogenesis (Vignuzzi et al., 2006). Another possibility is that individual mutations alone do not alter the phenotype of the virus, but instead multiple mutations act cooperatively to modulate virus replication and pathogenesis (Davis et al., 2007). The relative contribution of individual variants carrying specific (both individual and multiple) mutations implicated as important for host adaptation in our study versus that of emergent virus quasispecies remains to be tested in future studies, particularly since both scenarios have been shown to influence virulence of WNV (Jerzak et al., 2007).

In summary, the work in this paper has provided evidence that, in addition to the well known role of the E protein in host tropism, the M, NS3, NS4A and NS4B proteins may be viral determinants of host-specific replication. In particular, we suggest that the mutations identified in ISEp20 are not simply determinants of replication, but may be specific determinants of neuroinvasion. Because of this observation, the LGTV variants described here represent a unique set of viruses that have a defined yet limited number of mutations. Thus, these viruses can be used to direct studies using reverse genetics to determine the precise roles of individual mutations in host-specific replication and pathogenesis. This will provide insight into the functions of these proteins in virus replication in the two host systems.

Materials and methods

Description of cells, viruses and animals

Mouse neuroblastoma cells (MNB) or African green monkey kidney cells (Vero; ECACC) were cultured in Dulbecco's minimal essential medium (DMEM) supplemented with 10% fetal calf serum (FCS), 1% glutamine, and 50 μg/ml gentamicin at 37 °C in 5% CO_2. ISE6 cells, a cell line derived from *I. scapularis* embryonated eggs (a gift from Dr.

Timothy Kurtti, University of Minnesota) were cultured as previously described (Munderloh et al., 1994).

A Vero cell-derived virus stock of Langat virus (LGTV) strain TP21 was provided by Dr. Alexander Pletnev (NIAID, NIH) (Pletnev and Men, 1998). The virus was further propagated in Vero cells using a multiplicity of infection (MOI) of 0.005 (Campbell and Pletnev, 2000; Pletnev and Men, 1998).

Virus was titered in Vero cells by immunofocus forming assay (Blaney et al., 2001; Ishimine et al., 1987). Twenty-four well plates were seeded with 1×10^5 cells in complete DMEM. Virus prepared in 10-fold serial dilutions in complete DMEM was adsorbed for 1 h at 37 °C in 5% CO_2. The inoculum was removed and cells were washed with Dulbecco's phosphate-buffered saline (DPBS). Cells were then overlaid with 0.8% methylcellulose in DMEM with 2% FCS. Following incubation for 4 days at 37 °C in 5% CO_2, cell monolayers were fixed with 100% methanol for 30 min at room temperature. Cells were rinsed twice with phosphate-buffered saline (PBS) and blocked with OptiMEM for 10 min at room temperature. Next, the cells were incubated with a polyclonal mouse antibody cross-reactive to LGTV (hyperimmune mouse ascites fluid, clone Russian Spring Summer Encephalitis (RSSE) VR79; ATCC) at a 1:1000 dilution in OptiMEM for 1 h at 37 °C. Following two PBS washes and one OptiMEM wash, the secondary antibody (goat anti-mouse peroxidase-labeled polymer; DAKO Envision Systems) was applied at a 1:10 dilution in OptiMEM and incubated for 1 h at 37 °C. Focus forming units were visualized using a freshly prepared peroxidase substrate containing 0.4 mg/ml of 3,3′ diaminobenzidine and 0.0135% H_2O_2 in PBS.

Adult C57Bl/6 mice were purchased from Jackson Laboratory and bred at Rocky Mountain Laboratory (RML). All experiments were performed under protocols approved by the RML Institutional Animal Care and Use Committee.

Development of cell-derived virus variants

TP21 was plaque purified three times in Vero cells. Briefly, 10 fold serial dilutions were inoculated onto confluent Vero cell monolayers in 6 well plates. Following adsorption for 1 h at 37 °C in 5% CO_2, the monolayers were washed twice with DPBS and overlaid with 0.34% SeaKem agarose in minimal essential medium containing 5% FCS. After 7 days, plaques were visualized by vital staining with 0.1% Neutral Red for 3 h. Using a 200 µl pipette tip, plaques were collected and resuspended in 500 µl fresh media. The plaque-containing suspension was then used to inoculate a 35 mm culture dish containing a confluent monolayer of Vero cells. Infections continued until 90% cytopathic effect (CPE) was observed. Virus supernatant was cleared of cellular debris by centrifugation at 524 ×g for 5 min at 4 °C. The cleared supernatant was used for the next round of plaque purification. Following the third round of purification, a stock derived from plaque N6-1 (GenBank accession no. EU790644), denoted as TP21pp, was expanded in Vero cells and titered using the immunofocus forming assay (Blaney et al., 2001; Ishimine et al., 1987).

Virus variants were derived by 20 serial passages of TP21pp in either MNB or ISE6 cell lines. ISE6 cells were seeded at 2×10^6 cells in a 12.5 cm^2 flask. Using an MOI of 0.01, the virus was adsorbed for 1 h and then the cells were washed twice with PBS. Following addition of 3 ml culture media, the infection continued at 34 °C with no additional CO_2. Since infection of ISE6 cells with LGTV is persistent with no obvious CPE, we determined that the highest virus titer in the supernatant was obtained at 4 dpi (data not shown). Thus, supernatants were harvested at this time point for the subsequent passage. Infections used 1/8 volume of cleared supernatant from the previous passage. Following the 20th passage, a viral stock was propagated in ISE6 and titered in Vero cells utilizing the immunofocus forming assay. The virus derived following 20 passages in ISE6 cells was designated as ISEp20.

MNB cells were seeded at 7×10^5 cells in a 12.5 cm^2 flask and were initially infected at an MOI of 0.01. The virus was adsorbed for 1 h and then the cells were washed twice with PBS. Infections of MNB cells continued at 37 °C with 5% CO_2 until 90% CPE was observed. Subsequent infections used 1/8 volume of cleared supernatant from the previous infection. After 20 passages, a viral stock was propagated in MNB cells and virus titers were determined in Vero cells utilizing the immunofocus forming assay. This virus was termed MNBp20.

The mean focus size and standard error were obtained from 10 well isolated foci. Statistical significance of the focus size was determined by one-way ANOVA with Tukey post test.

Evaluation of virus replication in cell culture

Intracellular RNA replication was measured by quantitative real-time RT-PCR. Briefly, 96 well plates were seeded with MNB or ISE6 cells at 2×10^4 or 4×10^4 cells per well, respectively. Cells were infected in triplicate with the different viruses at an MOI of 0.01. The virus was adsorbed for 1 h at 4 °C and then washed two times with PBS. Following addition of appropriate growth media, the cells were incubated either at 37 °C with 5% CO_2 (MNB cells) or at 34 °C (ISE6 cells). RNA was isolated at indicated time points post infection using the RNeasy 96 kit (Qiagen).

Triplicate real-time PCR reactions were completed in a 20 µl volume using the CellsDirect Superscript™ III Platinum® One-Step qRT-PCR kit (Invitrogen). The reactions contained 2 µl of RNA and either 1× of the eukaryotic 18 s rRNA endogenous control VIC/TAMRA probe, primer limited mix (Applied Biosystems) or 200 nM of both the forward and reverse primer and 300 nM of the probe for detecting LGTV RNA and *I. scapularis* 16 s rRNA. *I. scapularis* 16 s rRNA was used as the endogenous control for the ISE6 cell line. The custom primers and probes used for detecting LGTV RNA (GenBank accession no. AF253419) and the *I. scapularis* 16 s rRNA (GenBank accession no. AF549857) were designed using the Primer Express software version 2.0 (Applied Biosystems). Positive sense RNA strand of LGTV was detected using forward primer LGTV911F (GGATTGTTGCCCAG-GATTCTC), reverse primer LGTV991R (TTCCAGGTGGGTGCATCTC), and probe LGTV951FAMT (6FAM-CATTGGCACCGGCCTACGCGT-TAMRA). *I. scapularis* 16 s rRNA was detected using forward primer 78IS16sF (GTCGCAAACTATTTTATCTATATGAACTATCC), reverse primer 170IS16sR (AAGTTCCGTTTTTAGCGATTAAATG), and probe 114IS16s-VICMGB (VIC-TTATTACGCTGTTATCCCTAGAGTA-MGB). RNA was analyzed with the ABI PRISM 7900HT sequence detection system using the SDS2.3 software (Applied Biosystems).

Viral RNA was quantified by the relative standard curve method (Applied Biosystems User Bulletin #2). LGTV cDNA from nucleotide 692-1184 (GenBank accession no. AF253420) was cloned into the pCR®II vector and transcribed by T7 polymerase using the MEGAscript high yield transcription kit (Ambion). We used 10 fold serial dilutions (ranging from 2×10^7 to 2×10^2 genome copies) of *in vitro* transcribed RNA to generate a standard curve for the positive sense strand of LGTV. For development of the 16 s rRNA and 18 s rRNA standard curves, total RNA was isolated from 4×10^6 ISE6 cells or 1×10^6 Vero cells using the RNEasy mini kit as per manufacturer's instruction (Qiagen) and ten fold serial dilutions from 1:10 to 1:1000000 were performed on the RNA. To determine the fold difference, the amount of viral RNA was normalized to the *I. scapularis* 16 s rRNA or the eukaryotic 18 s rRNA at each corresponding time point and 0 hours post infection (hpi) was used as the reference point.

Pathogenicity studies in mice

To evaluate differences in pathogenicity of the virus variants, 2 or 3 week old mice were either inoculated intracranially (IC) with 1×10^2 ffu or intraperitoneally (IP) with 1×10^3 ffu. Mice were observed daily for signs of disease which include weight loss, ruffled fur,

hunchback posture, loss of balance, and hind-limb paralysis (Holbrook et al., 2005; Seamer and Randles, 1967). Animals demonstrating hind-limb paralysis were considered terminal. The animals were anesthetized with isoflurane and were exsanguinated by transcardial perfusion with 20 ml of PBS. The brain was removed and bisected along the sagittal suture. Half of the brain was stored in RNA Later (Invitrogen) until RNA extraction was performed. A 10% brain homogenate in complete DMEM was created with half of the brain using the Omni TH homogenizer with the soft tissue disposable tips (Omni International).

Mice living 28 days post infection (dpi) were considered to have survived the infection. Serum was collected from these mice by retro-orbital bleed and mice were then anesthetized with isoflurane and exsanguinated and processed as described above. To confirm subclinical infections in mice surviving 28 dpi, the sera were tested for the presence of LGTV-specific antibodies by enzyme-linked immunosorbent assay (ELISA) as previously described (Mitzel et al., 2007). Survival curves were generated by the Kaplan–Meier method and the data sets were compared by the log-rank test using GraphPad Prism®4 software. Statistical significance was determined using the log-rank test and Geham–Breslow–Wilcoxon test.

Genome sequencing

Nucleotide sequence of the viral genome was obtained from RNA isolated from virus stocks or from brains of moribund mice. Following the manufacturer's protocol for large sample volumes from the QIAamp Viral RNA mini kit (Qiagen), viral RNA was isolated from 560 µl of the virus stocks. To isolate total RNA from brains of moribund C57Bl/6 mice, the mice were deeply anesthetized with isoflurane and exsanguinated by transcardial perfusion as noted above. The brain was removed and homogenized in 4 ml of RLT Buffer (Qiagen) using the Omni TH homogenizer. Total RNA was isolated using the RNeasy midi kit (Qiagen) according to the manufacturer's instructions.

To sequence the virus genome, 99.3% of the genome was divided into 6 overlapping segments of about 2500 nucleotides and complementary DNA (cDNA) was created using SuperScript III One-Step RT-PCR System with Platinum Taq DNA Polymerase (Invitrogen). The RT-PCR products were purified using one of two methods: QIAquick PCR Purification Kit (Qiagen) or by gel extraction using GenElute™ Minus EtBr Spin Columns (Sigma) following the manufactures recommendations. Purified cDNA was sequenced using a combination of 65 forward and reverse overlapping primers. Sequencing primers were designed using MacVector software (Accelrys Inc.). Primers longer than 18 nucleotides with melting temperatures of 60 °C or higher were selected. Primer sequences are available upon request. Sequence reactions consisted of 45 ng purified cDNA, 2.4 pmol primer, and 3 µl of ABI Terminator Ready Reaction Mix v3.1, in 15 µl. Generation of fluorescently-labeled extension products and their subsequent purification (Centri-Sep, Princeton Separations) were conducted as recommended by Applied Biosystems (ABI's BigDye® Terminator v3.1 Cycle Sequencing Kit Protocol, P/N 4337035). Reactions were run on an ABI 3730XL instrument (Applied Biosystems, Inc.). Sequence was analyzed using SeqMan, Editseq (DNAStar Lasergene) and Sequencher 4.6 software.

Sequence of the 5′ UTR was obtained by performing RNA ligase-mediated rapid amplification of the cDNA ends (RLM-RACE) using the GeneRacer™ kit (Invitrogen). The manufacturer's protocol was slightly modified by performing incubations at 95 °C for 5 min to relax RNA secondary structures. The RML-RACE product was then sequenced following either QIAQuick PCR purification or TA cloning into the pCR®4-TOPO® vector and transformation into TOP10 cells (Invitrogen). For bacterial clones, the DNA was purified using the Qiaprep Spin miniprep kit (Qiagen). DNA was sequenced as described above using either 210 ng of cDNA from plasmid purification or 9 ng of the QIAquick purified RLM-RACE product.

Sequence alignment and structural modeling

The amino acid sequences from the E protein of ISEp20 and Western TBEV (Neudorfl strain; GenBank accession no. NP_775503) or from NS3 of ISEp20 and YFV (GenBank accession no. NP_776005) were aligned using the Clustal W algorithm using DNAStar lasergene 7 MegAlign program. Amino acid changes in ISEp20 following adaptation to cells or following passage in mice were modelled to homologous residues of the TBEV E structure (Protein Data Bank ID. 1SVB) or to homologous amino acids of the YFV NS3 structure (Protein Data Bank ID. 1YMF) using PyMol.

Acknowledgments

The authors thank Kent Barbian, Stacy Ricklefs, Julia Marie and Kimmo Virtaneva from the Genomics Unit Research Technologies Section for their technical support and advice, Drs. John Portis, Shelly Robertson, Kristin McNally, and Travis Taylor for the critical review of the manuscript, and Gary Hettrick and Anita Mora for their graphical expertise. This research was supported by the intramural research program of the National Institutes of Health, National Institute of Allergy and Infectious Diseases.

References

Aaskov, J., Buzacott, K., Thu, H.M., Lowry, K., Holmes, E.C., 2006. Long-term transmission of defective RNA viruses in humans and Aedes mosquitoes. Science 311, 236–238.

Alvarez, D.E., De Lella Ezcurra, A.L., Fucito, S., Gamarnik, A.V., 2005. Role of RNA structures present at the 3′UTR of dengue virus on translation, RNA synthesis, and viral replication. Virology 339, 200–212.

Blaney Jr., J.E., Johnson, D.H., Firestone, C.Y., Hanson, C.T., Murphy, B.R., Whitehead, S.S., 2001. Chemical mutagenesis of dengue virus type 4 yields mutant viruses which are temperature sensitive in vero cells or human liver cells and attenuated in mice. J. Virol. 75, 9731–9740.

Blaney Jr., J.E., Johnson, D.H., Manipon, G.G., Firestone, C.Y., Hanson, C.T., Murphy, B.R., Whitehead, S.S., 2002. Genetic basis of attenuation of dengue virus type 4 small plaque mutants with restricted replication in suckling mice and in SCID mice transplanted with human liver cells. Virology 300, 125–139.

Bryant, J.E., Vasconcelos, P.F., Rijnbrand, R.C., Mutebi, J.P., Higgs, S., Barrett, A.D., 2005. Size heterogeneity in the 3′ noncoding region of South American isolates of yellow fever virus. J. Virol. 79, 3807–3821.

Butrapet, S., Huang, C.Y., Pierro, D.J., Bhamarapravati, N., Gubler, D.J., Kinney, R.M., 2000. Attenuation markers of a candidate dengue type 2 vaccine virus, strain 16681 (PDK-53), are defined by mutations in the 5′ noncoding region and nonstructural proteins 1 and 3. J. Virol. 74, 3011–3019.

Campbell, M.S., Pletnev, A.G., 2000. Infectious cDNA clones of Langat tick-borne flavivirus that differ from their parent in peripheral neurovirulence. Virology 269, 225–237.

Chernesky, M.A., McLean, D.M., 1969. Localization of Powassan virus in Dermacentor andersoni ticks by immunofluorescence. Can. J. Microbiol. 15, 1399–1408.

Chiou, S.S., Chen, W.J., 2001. Mutations in the NS3 gene and 3′-NCR of Japanese encephalitis virus isolated from an unconventional ecosystem and implications for natural attenuation of the virus. Virology 289, 129–136.

Ciota, A.T., Lovelace, A.O., Ngo, K.A., Le, A.N., Maffei, J.G., Franke, M.A., Payne, A.F., Jones, S.A., Kauffman, E.B., Kramer, L.D., 2007a. Cell-specific adaptation of two flaviviruses following serial passage in mosquito cell culture. Virology 357, 165–174.

Ciota, A.T., Ngo, K.A., Lovelace, A.O., Payne, A.F., Zhou, Y., Shi, P.Y., Kramer, L.D., 2007b. Role of the mutant spectrum in adaptation and replication of West Nile virus. J. Gen. Virol. 88, 865–874.

Costero, A., Grayson, M.A., 1996. Experimental transmission of Powassan virus (Flaviviridae) by Ixodes scapularis ticks (Acari:Ixodidae). Am. J. Trop. Med. Hyg. 55, 536–546.

Davis, C.T., Galbraith, S.E., Zhang, S., Whiteman, M.C., Li, L., Kinney, R.M., Barrett, A.D., 2007. A combination of naturally occurring mutations in North American West Nile virus nonstructural protein genes and in the 3′ untranslated region alters virus phenotype. J. Virol. 81, 6111–6116.

Dzhivanian, T.I., Korolev, M.B., Karganova, G.G., Lisak, V.M., Kashtanova, G.M., 1988. [Changes in the host-dependent characteristics of the tick-borne encephalitis virus during its adaptation to ticks and its readaptation to white mice]. Vopr. Virusol. 33, 589–595.

Gritsun, T.S., Gould, E.A., 2006. Direct repeats in the 3′ untranslated regions of mosquito-borne flaviviruses: possible implications for virus transmission. J. Gen. Virol. 87, 3297–3305.

Gritsun, T.S., Lashkevich, V.A., Gould, E.A., 2003. Tick-borne encephalitis. Antivir. Res. 57, 129–146.

Holbrook, M.R., Aronson, J.F., Campbell, G.A., Jones, S., Feldmann, H., Barrett, A.D., 2005. An animal model for the tickborne flavivirus-Omsk hemorrhagic fever virus. J. Infect. Dis. 191, 100–108.

Ishimine, T., Tadano, M., Fukunaga, T., Okuno, Y., 1987. An improved micromethod for infectivity assays and neutralization tests of dengue viruses. Biken J. 30, 39–44.

Jerzak, G.V., Bernard, K., Kramer, L.D., Shi, P.Y., Ebel, G.D., 2007. The West Nile virus mutant spectrum is host-dependant and a determinant of mortality in mice. Virology 360, 469–476.

Kaluzova, M., Eleckova, E., Zuffova, E., Pastorek, J., Kaluz, S., Kozuch, O., Labuda, M., 1994. Reverted virulence of attenuated tick-borne encephalitis virus mutant is not accompanied with the changes in deduced viral envelope protein amino acid sequence. Acta Virol. 38, 133–140.

Labuda, M., Jiang, W.R., Kaluzova, M., Kozuch, O., Nuttall, P.A., Weismann, P., Eleckova, E., Zuffova, E., Gould, E.A., 1994. Change in phenotype of tick-borne encephalitis virus following passage in Ixodes ricinus ticks and associated amino acid substitution in the envelope protein. Virus Res. 31, 305–315.

Lee, E., Hall, R.A., Lobigs, M., 2004. Common E protein determinants for attenuation of glycosaminoglycan-binding variants of Japanese encephalitis and West Nile viruses. J. Virol. 78, 8271–8280.

Leonova, G.N., 1997. Tick-borne Encephalitis in Primorskii Region: Virological, Ecological, and Epidemiological Aspects. Dal'nauka Press, Vladivostock.

Lindenbach, B.D., Rice, C.M., 2001. Flaviviridae: The Viruses and Their Replication. In: Knipe, D.M., Howley, P.M. (Eds.), Fields Virology. Lippincott Williams and Wilkins, Philadelphia, pp. 991–1042.

Maier, C.C., Delagrave, S., Zhang, Z.X., Brown, N., Monath, T.P., Pugachev, K.V., Guirakhoo, F., 2007. A single M protein mutation affects the acid inactivation threshold and growth kinetics of a chimeric flavivirus. Virology 362, 468–474.

Mitzel, D.N., Wolfinbarger, J.B., Long, R.D., Masnick, M., Best, S.M., Bloom, M.E., 2007. Tick-borne flavivirus infection in Ixodes scapularis larvae: development of a novel method for synchronous viral infection of ticks. Virology 365, 410–418.

Munderloh, U.G., Liu, Y., Wang, M., Chen, C., Kurtti, T.J., 1994. Establishment, maintenance and description of cell lines from the tick Ixodes scapularis. J. Parasitol. 80, 533–543.

Nuttall, P.A., Labuda, M., 1994. Tick-borne Encephalitis Subgroup. In: Sonenshine, D.E., Mather, T.M. (Eds.), Ecological Dynamics of Tick-borne Zoonoses. Oxford Press, New York, pp. 351–391.

Nuttall, P.A., Labuda, M., 2003. Dynamics of infection in tick vectors and at the tick-host interface. Adv. Virus Res. 60, 233–272.

Nuttall, P.A., Jones, L.D., Davies, C.R., 1991. The role of arthropod vectors in arbovirus evolution. Adv. Dis. Vector Res. 15–45.

Pletnev, A.G., 2001. Infectious cDNA clone of attenuated Langat tick-borne flavivirus (strain E5) and a 3′ deletion mutant constructed from it exhibit decreased neuroinvasiveness in immunodeficient mice. Virology 282, 288–300.

Pletnev, A.G., Men, R., 1998. Attenuation of the Langat tick-borne flavivirus by chimerization with mosquito-borne flavivirus dengue type 4. Proc. Natl. Acad. Sci. U. S. A. 95, 1746–1751.

Puig-Basagoiti, F., Tilgner, M., Bennett, C.J., Zhou, Y., Munoz-Jordan, J.L., Garcia-Sastre, A., Bernard, K.A., Shi, P.Y., 2007. A mouse cell-adapted NS4B mutation attenuates West Nile virus RNA synthesis. Virology 361, 229–241.

Rey, F.A., Heinz, F.X., Mandl, C., Kunz, C., Harrison, S.C., 1995. The envelope glycoprotein from tick-borne encephalitis virus at 2 A resolution. Nature 375, 291–298.

Romanova, L.I., Gmyl, A.P., Dzhivanian, T.I., Bakhmutov, D.V., Lukashev, A.N., Gmyl, L.V., Rumyantsev, A.A., Burenkova, L.A., Lashkevich, V.A., Karganova, G.G., 2007. Microevolution of tick-borne encephalitis virus in course of host alternation. Virology 362, 75–84.

Rossi, S.L., Fayzulin, R., Dewsbury, N., Bourne, N., Mason, P.W., 2007. Mutations in West Nile virus nonstructural proteins that facilitate replicon persistence in vitro attenuate virus replication in vitro and in vivo. Virology 364, 184–195.

Rumyantsev, A.A., Chanock, R.M., Murphy, B.R., Pletnev, A.G., 2006a. Comparison of live and inactivated tick-borne encephalitis virus vaccines for safety, immunogenicity and efficacy in rhesus monkeys. Vaccine 24, 133–143.

Rumyantsev, A.A., Murphy, B.R., Pletnev, A.G., 2006b. A tick-borne Langat virus mutant that is temperature sensitive and host range restricted in neuroblastoma cells and lacks neuroinvasiveness for immunodeficient mice. J. Virol. 80, 1427–1439.

Seamer, J., Randles, W.J., 1967. The course of Langat virus infection in mice. Br. J. Exp. Pathol. 48, 403–410.

Vignuzzi, M., Stone, J.K., Arnold, J.J., Cameron, C.E., Andino, R., 2006. Quasispecies diversity determines pathogenesis through cooperative interactions in a viral population. Nature 439, 344–348.

Wicker, J.A., Whiteman, M.C., Beasley, D.W., Davis, C.T., Zhang, S., Schneider, B.S., Higgs, S., Kinney, R.M., Barrett, A.D., 2006. A single amino acid substitution in the central portion of the West Nile virus NS4B protein confers a highly attenuated phenotype in mice. Virology 349, 245–253.

Wu, J., Bera, A.K., Kuhn, R.J., Smith, J.L., 2005. Structure of the Flavivirus helicase: implications for catalytic activity, protein interactions, and proteolytic processing. J. Virol. 79, 10268–10277.

Yamashita, T., Unno, H., Mori, Y., Tani, H., Moriishi, K., Takamizawa, A., Agoh, M., Tsukihara, T., Matsuura, Y., 2008. Crystal structure of the catalytic domain of Japanese encephalitis virus NS3 helicase/nucleoside triphosphatase at a resolution of 1.8 A. Virology 373, 426–436.

Yu, L., Markoff, L., 2005. The topology of bulges in the long stem of the flavivirus 3′ stem-loop is a major determinant of RNA replication competence. J. Virol. 79, 2309–2324.

Zhang, W., Chipman, P.R., Corver, J., Johnson, P.R., Zhang, Y., Mukhopadhyay, S., Baker, T.S., Strauss, J.H., Rossmann, M.G., Kuhn, R.J., 2003. Visualization of membrane protein domains by cryo-electron microscopy of dengue virus. Nat. Struct. Biol. 10, 907–912.

Zeng, L., Falgout, B., Markoff, L., 1998. Identification of specific nucleotide sequences within the conserved 3′-SL in the dengue type 2 virus genome required for replication. J. Virol. 72, 7510–7522.